Cerebral Cortex, March 2017;27:2249–2259

doi:10.1093/cercor/bhw055
Advance Access Publication Date: 22 March 2016
Original Article

ORIGINAL ARTICLE

Altered Brain Network Segregation in Fragile X Syndrome Revealed by Structural Connectomics

Jennifer Lynn Bruno[1], S. M. Hadi Hosseini[1], Manish Saggar[1], Eve-Marie Quintin[2], Mira Michelle Raman[1] and Allan L. Reiss[1,3,4]

[1]Department of Psychiatry, Center for Interdisciplinary Brain Sciences Research, Stanford, CA 94305-5795, USA, [2]School and Applied Child Psychology Program, McGill University, Montreal, QC, Canada H3A 1Y2, [3]Department of Radiology and [4]Department of Pediatrics, Stanford University, Stanford, CA 94305, USA

Address correspondence to Jennifer Lynn Bruno, Center for Interdisciplinary Brain Sciences Research, Stanford University, 401 Quarry Road, Stanford, CA 94305-5795, USA. Email: bruno.jennifer@gmail.com

Abstract

Fragile X syndrome (FXS), the most common inherited cause of intellectual disability and autism spectrum disorder, is associated with significant behavioral, social, and neurocognitive deficits. Understanding structural brain network topology in FXS provides an important link between neurobiological and behavioral/cognitive symptoms of this disorder. We investigated the connectome via whole-brain structural networks created from group-level morphological correlations. Participants included 100 individuals: 50 with FXS and 50 with typical development, age 11–23 years. Results indicated alterations in topological properties of structural brain networks in individuals with FXS. Significantly reduced small-world index indicates a shift in the balance between network segregation and integration and significantly reduced clustering coefficient suggests that reduced local segregation shifted this balance. Caudate and amygdala were less interactive in the FXS network further highlighting the importance of subcortical region alterations in the neurobiological signature of FXS. Modularity analysis indicates that FXS and typically developing groups' networks decompose into different sets of interconnected sub networks, potentially indicative of aberrant local interconnectivity in individuals with FXS. These findings advance our understanding of the effects of fragile X mental retardation protein on large-scale brain networks and could be used to develop a connectome-level biological signature for FXS.

Key words: connectome, graph theory, fragile X syndrome, large-scale brain networks, small-world, structural correlation networks

Introduction

Fragile X syndrome (FXS), the leading known cause of inherited intellectual disability, is associated with a host of behavioral, social, and neurocognitive deficits attributed to limited or lack of the fragile X mental retardation protein (FMRP) (Irwin et al. 2001). FMRP plays a critical regulatory role in synaptic plasticity and dendritic pruning (Swanger and Bassell 2011). Reduced FMRP is associated with cognitive impairment (Hall et al. 2008) as well as social deficits that overlap with characteristics of autism spectrum disorders (ASDs) (Gabis et al. 2011).

Neuroimaging studies of individuals with FXS have described aberrant function and morphology for regions underlying cognitive and social functioning. Structural neuroimaging demonstrates regional alterations in gray matter, including enlarged caudate and thalamus volumes as well as decreased cerebellar vermis, amygdala, and insula volumes (Lee et al. 2007; Gothelf et al. 2008; Bray et al. 2011; Cohen et al. 2011). Functional imaging indicates differences within regions involved with social processing (Bruno et al. 2014) and executive functions such as response inhibition (Menon et al. 2004). Evidence from the fragile X mouse

model suggests deficits in neural circuitry (Gonçalves et al. 2013) and white matter abnormalities have been reported in humans with FXS in frontostriatal pathways (Barnea-Goraly et al. 2003) as well as in the inferior longitudinal fasciculus, a major anterior/posterior association pathway (Green et al. 2015). Accordingly, a recent study demonstrated alterations in resting state functional connectivity associated with FXS (Hall et al. 2013). Essentially, neuroimaging studies demonstrate system-wide neurobiological abnormalities in individuals FXS, indicating alterations in large-scale brain networks.

A promising new method for examining large-scale brain networks (i.e., the connectome) involves examining group-level morphological correlations (e.g., regional thickness and volume correlations) (He et al. 2007). Population covariance of regional brain morphology reflects synchronized maturational changes in connected regions over the course of years (Alexander-Bloch et al. 2013). Structural networks constructed as such follow small-world characteristics—an architecture that optimizes local and global information processing. Within the framework of graph theoretical analysis, structural correlation networks correspond with functional networks (Hosseini and Kesler 2013a) and anatomically based networks created via white matter tractography (He et al. 2007), although they represent unique meaningful information as well (Gong et al. 2012).

Despite the burgeoning field of network dynamics, no study to date has utilized a graph theoretical approach to investigate brain differences associated with FXS. Research in carriers of the *FMR1* premutation suggests that condition is associated with regional disruption of diffusion network measures (Leow et al. 2014) but, because premutation carriers do not have severely altered FMRP levels, we would expect quite different patterns of network disruption among individuals with FXS.

The present study investigated structural brain network topology in males and females with FXS using structural magnetic resonance imaging (MRI) and graph theoretical analysis. Females and males with FXS are known to have reduced FMRP, and disadvantageous cognitive, behavioral, and neurobiological symptoms although symptom severity is generally less among females, attributed to the presence of a second unaffected X chromosome (Reiss and Dant 2003). We hypothesized that, given the distributed gray and white matter differences as well as the altered functional network differences reported previously, individuals with FXS would display aberrant structural correlation networks evidenced by altered global network organization, specifically, reduced small-worldness. Information about global-scale brain organization in FXS will enhance our understanding of the effects of FMRP on brain development. We also examined univariate group differences in cortical thickness and subcortical/cerebellar volume to put results in context with previous reports of regional structural differences.

Materials and Methods

Participants included 50 individuals with FXS (30 females) and an age-matched group of 50 typically developing (TD) participants (30 females), all between 11 and 23 years of age (Table 1). Due to the wide age range in our sample, we performed parallel analyses for a subgroup of individuals with a much narrower age range: 15–23 years ($n = 40$ FXS and 40 TD), which are presented in Supplementary Table 2.

For the FXS group genetic diagnoses were confirmed via Southern blot DNA analysis (>200 CGG repeats on the FMR1 gene and evidence of aberrant methylation). Three male participants demonstrated mosaicism indicated by the presence of an additional unmethylated fragment in the premutation range. Five individuals (2 females) had a history of seizures; none reported current seizure disorder. Fourteen individuals (6 females) were taking psychoactive medications including stimulants, selective serotonin reuptake inhibitors, and antiepileptics. Blood was drawn from each individual to estimate FMRP percentage. Analysis was based on the percentage of peripheral lymphocytes containing FMRP, as assessed by immunostaining techniques (Willemsen et al. 1997).

TD participants were excluded for the following: any known genetic condition, premature birth (<34 weeks), low birth weight (<2000 g), or any learning, developmental, psychiatric, neurological, or medical disorder. All participants were free from MRI contraindications, met screening criteria for the ability to tolerate MRI procedures (e.g., the ability to hold still and minimal sensitivity to loud noises) and were trained to hold motionless in the scanner. Participants were part of an ongoing longitudinal study (Bray et al. 2011) from which several other reports of T_1-weighted structural neuroimaging outcomes have been published (Lee et al. 2007; Gothelf et al. 2008; Cohen et al. 2011; Peng et al. 2014; Saggar et al. 2015). The present study is the first investigation to use multivariate analysis to characterize interaction among brain regions using this data with the exception of a recent methodological report from our group (Saggar et al. 2015) which used nearly the same dataset as described here (99% overlap in participants) but did not compare FXS and TD groups

From the larger longitudinal study, we selected MRI datasets for which participants were aged 11–23 years and for which strict image quality requirements were met. Image quality requirements included lack of artifacts induced by subject motion, blood flow, or wraparound and approximately 19% of scans in the longitudinal study were unusable due to such artifacts.

Participants were recruited across the USA and Canada through advertisements, referrals and word of mouth. Participants and/or their parents gave written informed consent and assent to participate and Stanford University's Institutional Review Board approved all protocols.

General intellectual functioning (IQ) was assessed via the Wechsler Abbreviated Scale for Intelligence (Wechsler 1997) (age ≥17 years) or the Wechsler Intelligence Scale for Children

Table 1 Participant characteristics

	FXS	TD	T	P
Participant characteristics				
N (*N* females)	50 (30 female)	50 (30 female)	–	–
Age (years)	17.47 (2.88)	17.66 (2.65)	0.35	>0.10
IQ	72.41 (20.24)	119.56 (13.96)	13.80	<0.001
Total brain volume (cc)	1232 (111)	1238 (92)	0.26	>0.10

Values are mean (standard deviation) unless otherwise noted. IQ = Wechsler full-scale intelligence quotient.

(Wechsler 1991) (age <17 years). Within the FXS group, adaptive behavior was assessed via the Aberrant Behavior Checklist–Community (ABC, Aman et al. 1995). Assessments were completed within 6 months of MR imaging for all participants except for 2 in the TD group for whom assessments were completed within 21 months. Sex differences in IQ, ABC, and FMRP were evaluated within the FXS group given the X linked nature of the disorder and the differences in symptom severity between sexes. Significant sex differences were found for IQ (male mean = 57.20, SD = 9.89, female mean = 81.21, SD = 19.81, $t = 5.59$, $P < 0.01$), ABC (male mean = 25.11, SD = 17.45, female mean = 11.43, SD = 16.14, $t = 2.76$, $P < 0.01$), and FMRP (male mean = 17.1, SD = 20.0, female mean = 55.3, SD = 19.2, $t = 6.93$, $P < 0.01$).

Image Acquisition and Processing

Anatomical T_1-weighted images were acquired at 1.5 T (General Electric, Stanford University). Repetition time = 35 ms, echo time = 6 ms, flip angle = 45°, slice thickness: 1.5–1.7 mm (adjusted to include the entire brain), in-plane resolution = 0.9375 × 0.9375 mm, and acquisition matrix = 256 × 192 mm, 124 contiguous coronal slices). FreeSurfer version 5 (http://surfer.nmr.mgh.harvard.edu/) was used to parcellate brains into 86 gray matter regions (68 cortical, 16 subcortical, 2 cerebellum, Supplementary Table 1), and compute measures of cortical thickness and subcortical/cerebellar volume. FreeSurfer is a surface based segmentation pipeline that preserves anatomical variation at the individual level and provides reliable segmentation of cortical, subcortical, and cerebellar structures (Dale et al. 1999). The FreeSurfer derived surfaces were examined and adjusted by editors with inter-rater reliability ≥0.95 using the methods described in the FS tutorial (http://surfer.nmr.mgh.harvard.edu/fswiki/FsTutorial) until the surfaces satisfactorily delineated both the grey/white boundary and pial surface.

We chose to use thickness as the metric for cortical regions of interest given the strong correspondence between thickness networks and anatomical connectivity (He et al. 2007; Bernhardt et al. 2011). Furthermore, cortical thickness may represent a superior endophenotype for neurogenetic syndromes when compared with cortical volume (Panizzon et al. 2009). Neurobiological differences found previously (Gothelf et al. 2008; Bray et al. 2011) necessitated including subcortical and cerebellar structures to understand network differences associated with FXS. Including cortical thickness and subcortical/cerebellar volumes is a strategy that has been utilized previously (Hosseini et al. 2013). The results of that study demonstrated that subcortical regions contribute important and meaningful additions to structural correlation networks and that these networks demonstrate small-world organization. Normalization was performed in 2 steps. First, regional measures were normalized to remove effects of overall brain size, sex and age using residuals from linear regression, as is common practice for graph theoretical analysis (Bernhardt et al. 2011; Alexander-Bloch et al. 2013). Second, we performed additional normalization on the residuals due to the different scale for cortical thickness (~2–4 mm) and subcortical/cerebellar volumes (several hundred mm^3). This was achieved by dividing the value for each region by the absolute value of the maximum residual for that region. The resulting values were between –1 and 1 for each region and could then be entered into the group-wise structural correlation network.

Creation of Structural Correlation Networks

A whole-brain structural correlation network was defined for each group as a set of nodes (86 gray matter regions) and edges (connections) (Fig. 1). The edges corresponded to group-wise correlations between the normalized thickness/volume of each brain region. For each group, an 86 × 86 association matrix R was generated with each entry r_{ij} equal to the Pearson correlation coefficient between normalized volume/thickness of regions i and j across participants in the group. Binary association matrices were used given the methodological concerns when comparing weighted matrices (Rubinov and Sporns 2011). Each matrix was thresholded to create a binary adjacency matrix A where a_{ij} was retained as an edge (set equal to 1) if r_{ij} was greater than a specific threshold T, and a_{ij} was not retained as an edge (set equal to 0) if r_{ij} was less than T. T was always greater than 0; thus, negative values for r_{ij} were set equal to 0. Diagonal elements of the association matrix were set equal to 0. The adjacency matrix A represented a binary undirected graph G in which regions i and j were connected if g_{ij} was equal to 1. Graph G had a network degree of E equal to the number of edges, and a network density (cost) of $D = E/[N_x(-1)]/2$ representing the ratio of existing edges relative to all possible edges.

Network Measures

Global and regional network measures included clustering coefficient, path length, small-worldness, degree, betweenness centrality, and modularity. Measures were defined as in previous studies (Bassett et al. 2008; Rubinov and Sporns 2010; Sporns 2011) and were quantified using Brain Connectivity Toolbox (Rubinov and Sporns 2010). Briefly, the clustering coefficient of a node is equal to the proportion of a node's neighbors that are also neighbors with each other. The clustering coefficient of a network is equal to the average of clustering coefficients across nodes and represents network segregation. The path length is equal to the minimum number of edges that separates a pair of nodes. The characteristic path length of a network is the average shortest path length between pairs of nodes in the network and represents network integration. Small-worldness is a property of organization common to brain and other large-scale complex biological networks that differentiates them from random networks, which do not display any systematic organization of nodes and edges. Small-world networks display greater clustering but similar path length relative to random networks. This organization represents an optimal balance between network segregation and integration (Watts and Strogatz 1998). The small-world index of a network was defined as the ratio of normalized clustering to normalized path length (Humphries et al. 2006).

Degree, a measure of the node's interaction within the network, is equal to the number of connections a node has with the rest of the network. Degree was calculated for each node in each network and was normalized by the mean network degree. Betweenness centrality is the fraction of all shortest paths in the network that pass through a given node. Hubs are the most globally interconnected regions in a network and were defined as a region whose nodal betweenness centrality was one standard deviation higher than the mean network betweenness (Hosseini, Hoeft, et al. 2012).

Modularity analysis identifies subdivisions (modules) in a network that have maximal within-module connections and minimal between-module links. This complex measure of network segregation quantifies the degree of subdivision within a network and the individual nodes that comprise a network's modular communities. GAT uses algorithms implemented in Brain Connectivity Toolbox (BCT) (Rubinov and Sporns 2010) to quantify modular structure. Specifically, the BCT implementation of Newman modularity detection algorithm (Newman

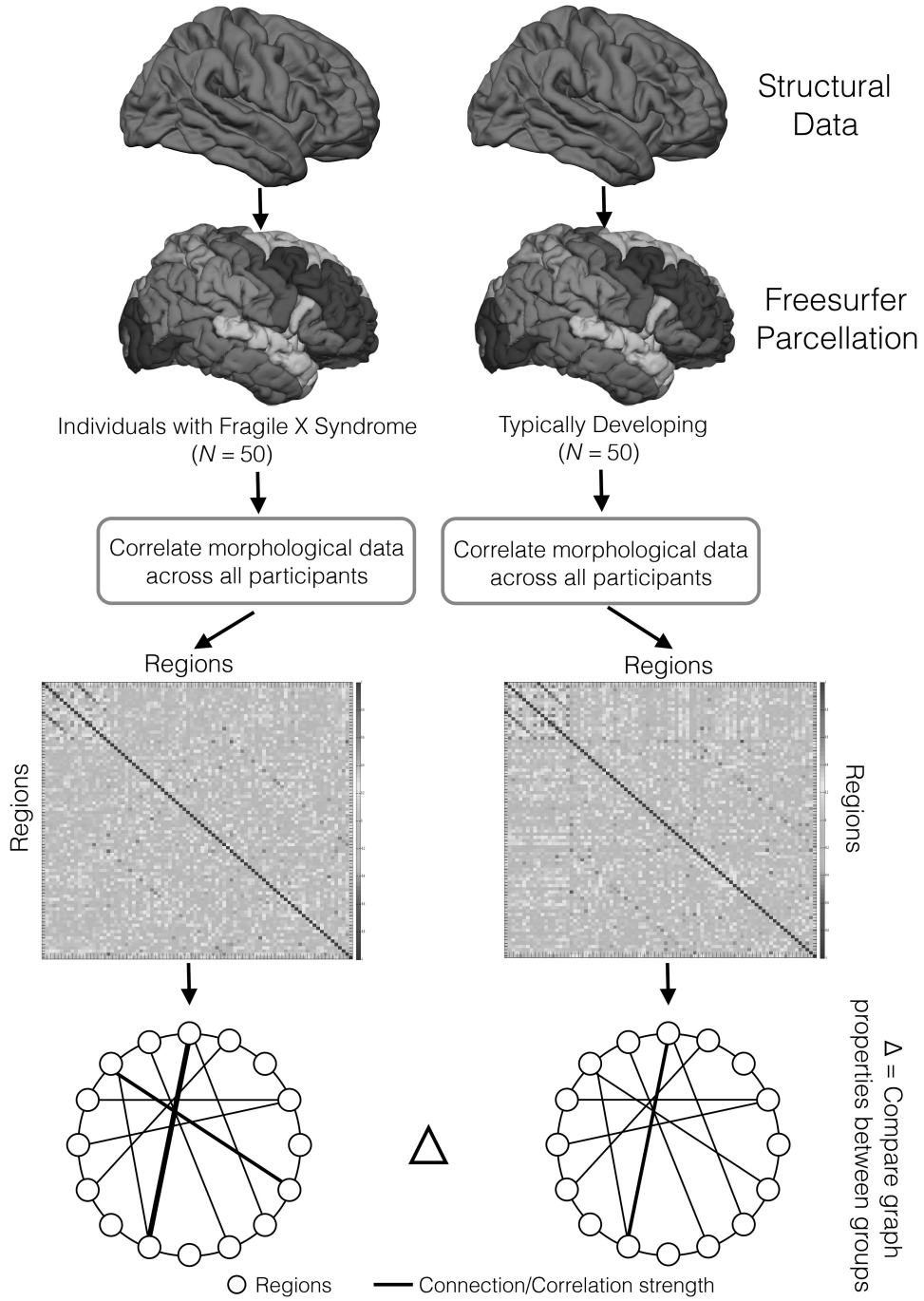

Figure 1. Creation of structural correlation networks. Flow chart describing creation of group-wise structural correlation networks.

2006) was used. The algorithm was run 100 times and the modular structure with the highest maximized modularity value was used as the representative modular structure for each group.

BrainNet viewer was used for network visualization (Xia et al. 2013).

Statistical Analysis of Networks

Comparison of Networks Between Groups

Our in-house Graph Analysis Toolbox (Hosseini, Hoeft, et al. 2012) was used to compare structural networks between-groups. Thresholding at an absolute value results in different numbers of nodes and degrees across groups, introducing a confound for between-group comparisons (Gong et al. 2012). To address this limitation, we examined graph metrics over a range of connection densities (K) in which graphs exhibited criteria of the small-world regime. The lower limit was consistently defined as a value where graphs were not fragmented (each node had at least one connection with another node). The choice for the upper limit is less obvious. One option is to use an upper limit of $K = 49\%$, a density at which connections are likely nonbiological (Kaiser and Hilgetag 2006). A second option is to use a value of K for which

sigma >1.2 (Bassett et al. 2008). We chose to examine network properties in parallel analyses over 2 density ranges to minimize bias in choice of density range and to confirm the stability of our results. The first range was set with 49% as the upper limit and the second with sigma >1.2 as the upper limit. We employed an area under a curve (AUC) summary measure (Hosseini, Hoeft, et al. 2012) for between-group comparisons across density steps equal to a 2% increase for each density range. AUC is less sensitive to thresholding and reduces the number of comparisons.

The topology of brain networks was evaluated by contrasting each group's network measures with mean values of random graphs having the same number of nodes, edges, and degree distribution (Hosseini and Kesler 2013b). Recent evidence suggests that networks constructed from correlations are inherently more clustered than are random networks and that correlation introduces an additive small-world organization to the network (Zalesky et al. 2012). To overcome this limitation, we generated random networks from covariance matrices that were matched to the distributional properties of the observed covariance matrix using the Hirschberger–Qi–Steuer algorithm (Hirschberger et al. 2007).

Nonparametric permutation testing (1000 repetitions) was used to determine the statistical significance of between-group differences (He et al. 2008; Hosseini, Hoeft, et al. 2012). Residual volumes/thickness for each participant were randomly reassigned to one of the 2 groups for each repetition; each randomized group had the same number of participants. Network measures were calculated for each network at each density and summarized using AUC (Hosseini, Koovakkattu, et al. 2012). Between-group differences in regional and global network measures for randomized groups were calculated creating a permutation distribution of between-group difference under the null hypothesis. The actual between-group difference in network measures was placed in the corresponding permutation distribution and a 2-tailed *P*-value was calculated based on percentile position. The statistical threshold for group difference in global network integrity was 0.05. For regional network differences the statistical threshold was 0.05 corrected for multiple comparisons using the false discovery rate (FDR). As stated above, global modularity was compared statistically but comparison of modularity assignments (i.e., which regions comprise each module in each group) and hub locations were considered qualitative. Group-wise modular structure was assessed at the minimum network density (0.07).

We compared the overall interregional correlation strength of thickness/volume between-groups. Correlation coefficients were converted to z values (Fisher's *r*-to-z) and a 2-sample *t*-test was used to examine group differences in mean overall correlation.

Univariate Statistical Analysis

Group differences in regional cortical thickness were assessed using Freesurfer's qdec, which fits a general linear model at each surface vertex. Surface smoothing was performed (10 mm full width at half-maximum Gaussian kernel) and results were thresholded at $P < 0.05$ corrected for multiple comparisons using Monte Carlo simulation. Subcortical/cerebellar volumes were compared using region of interest approach. The Bonferroni corrected threshold for volume differences was $P < 0.003$ (0.05/18 regions). All group comparisons were covaried for age, sex and in the case of volumetric measures, total brain volume. Cortical thickness is a local cytoarchitectural measure and, when compared regionally vertex-by-vertex, correction for influences of overall brain volume may not apply. Therefore, we performed parallel analyses of cortical thickness including a total brain covariate as recommended (O'Brien et al. 2011).

Results

IQ was lower for the FXS group relative to the TD group ($P < 0.01$) but the 2 groups did not differ on measured total brain volume ($P > 0.10$, Table 1).

Network Topology

There was no group difference in overall correlation strength ($P > 0.10$). FXS and TD groups displayed structural correlation networks with small-world properties at some network densities. Figure 2 illustrates network properties for each group at a broad range of densities (A) as well as group differences at all densities (B). The minimum network density for full connectivity for both groups was 0.075 and the maximum density at which small-world index was >1.2 was 0.17; thus the density ranges compared were [0.07–0.49] and [0.07–0.17]. With regards to our primary hypothesis, AUC comparison revealed reduced small-world index in the FXS group for both density ranges ($P = 0.006$ and $P = 0.002$, respectively). Reduced clustering ($P = 0.006$, $P = 0.002$), and marginally significantly reduced path length ($P = 0.050$, $P = 0.066$) were also present for both density ranges in the FXS group.

Regional Group Differences in Network Properties

The FXS group demonstrated lower degree in bilateral amygdala, bilateral caudate, left rostral anterior cingulate, and right temporal pole, for both density ranges (Table 2 and Fig. 3A).

Hubs and Modularity

FXS and TD groups displayed different network hub distributions (Table 2, Fig. 3B and C), results are presented for the first density range [0.07–0.49] for these qualitative analyses. Thirteen hubs were found in the FXS group (6 subcortical, 7 cortical) and 17 in TD group (4 subcortical, 13 cortical). Divergent hub locations were present in frontal, temporal parietal, and occipital cortical locations as well as subcortical structures. One hub location—the right amygdala—was common between the groups. The TD group displayed additional subcortical hubs in bilateral caudate whereas the FXS group displayed hubs in bilateral thalamus, accumbens, and right palladium.

The 2 groups did not differ on the modularity statistic for either density range ($P > 0.10$), but the FXS and TD groups' networks have different modular structures, especially with respect to the subcortical nodes (Fig. 3D and E). For the FXS group all but 2 of the subcortical nodes are included in a single module that does not include any cortical nodes (red module). In the TD group, the subcortical structures are part of several modules including cortical and subcortical structures (the yellow, dark blue, and green and orange modules). Supplementary Table 4 reports complete modularity assignments per group; additional visualizations of modularity are presented in Supplementary Figure 3 and Videos 1 and 2.

Reduced age Range Comparisons

The same pattern of group differences in global network measures was demonstrated in this reduced sample (Supplementary Table 2). Reduced small-world index and clustering were significant for the density range [0.07–0.17] and reached trend level for the range [0.07–0.49].

Group Differences in Cortical Thickness and Subcortical/Cerebellar Volume

The FXS groups displayed significantly greater cortical thickness in several large clusters spanning the occipital, temporal, and

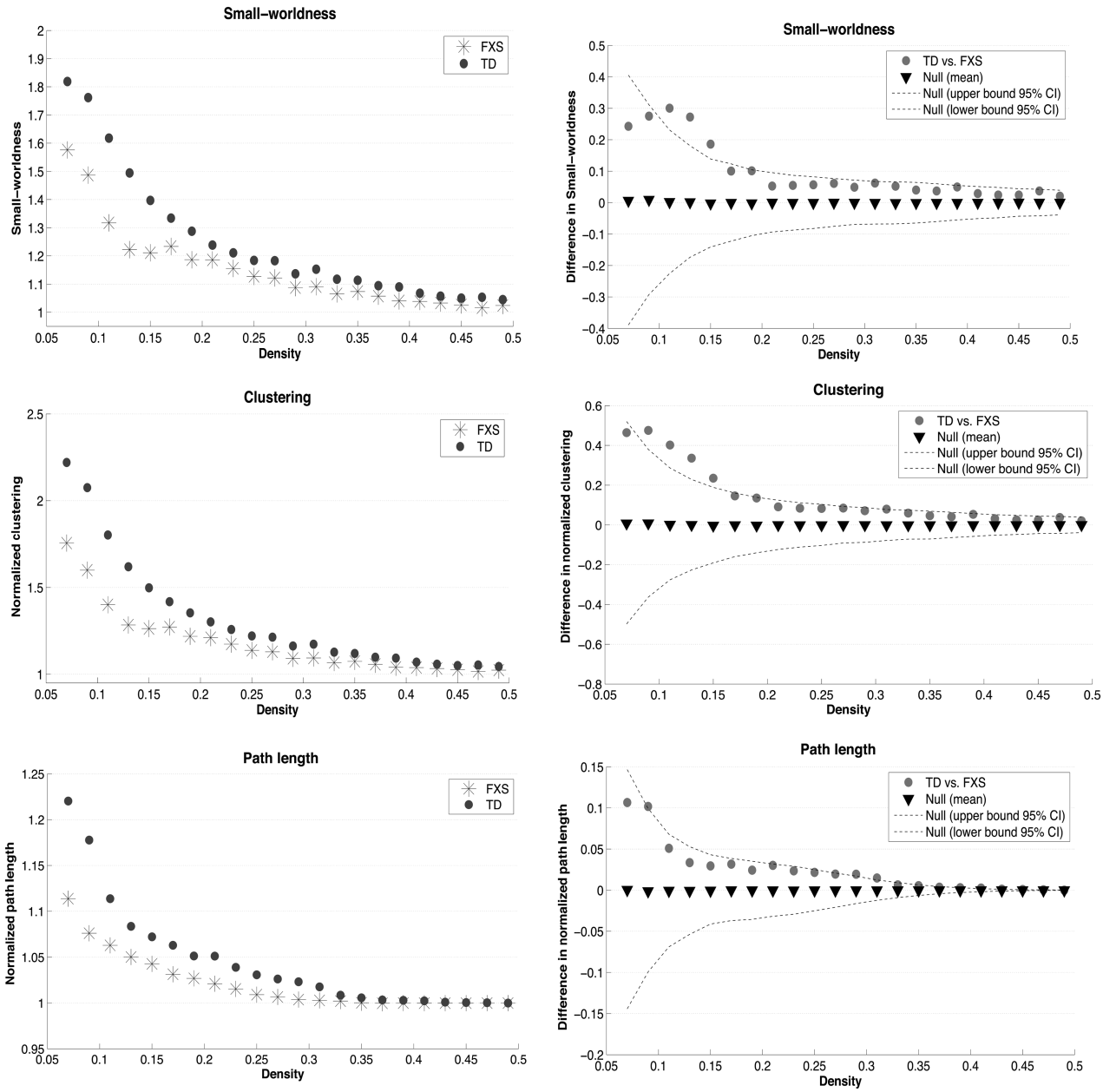

Figure 2. Global network measures. (*A*) Changes in global network measures as a function of network density. Data points represent group-level network summaries. (*B*) Between-group differences in global network measures.

frontal lobes (Table 3, Supplementary Fig. 1), and significantly enlarged bilateral caudate and left palladium volumes (Table 4). Cortical thickness results including the total brain covariate are presented in Supplementary Table 4 and Figure 2. These results are similar to those results not including this covariate yet the extent of significant clusters is reduced.

Discussion

We present results of the first study to investigate large-scale structural correlation network topology in individuals with FXS. When compared with individuals with TD, the FXS group demonstrated alterations in global topological properties including significantly reduced small-world index, suggesting a shift in the balance between network segregation and integration. Differences in regional network properties and modularity were consistent with previously reported neuroanatomical and neurofunctional abnormalities in individuals with FXS. Our results indicate that FXS is associated with differences across widespread and specific regions of the brain, and across multiple levels of network hierarchy. These results shed light on the effects of FMRP on the connectome and elucidate the altered network structure associated with FXS.

Brain networks, like other complex biological networks, have a small-world organization that balances network integration and segregation, maximizing efficient transfer of information while minimizing network cost (Watts and Strogatz 1998). Networks of both groups displayed small-world organization evidenced by higher clustering and comparable path length relative to random networks. However, the measure of small-worldness (the ratio of

Table 2 Regional group differences in degree and network hubs

TD > FXS	*P* value K = 0.07–0.49	*P* value K = 0.07–0.17
Group differences in degree		
Left amygdala	0.004	0.004
Right amygdala	0.002	0.03
Left caudate	0.008	<0.001
Right caudate	0.008	0.01
Left rostral anterior cingulate	0.03	0.032
Right temporal pole	0.036	0.024
Region name Network Hubs	**Hubs FXS**	**Hubs TD**
Caudate		Bilateral
Thalamus	Bilateral	
Pallidium	Right	
Amygdala	Right	Bilateral
Accumbens area	Bilateral	
Rostral anterior cingulate		Left
Caudal anterior cingulate	Right	
Isthmus cingulate		Right
Pars oppercularis	Left	
Parahippocampal		Right
Insula		Right
Transverse temporal		Left
Bank of superior temporal sulcus		Right
Superior temporal		Right
Middle Temporal		Left
Inferior temporal	Left	
Temporal pole		Right
Fusiform	Right	
Lateral orbitofronal		Bilateral
Rostral middle frontal	Right	
Lingual	Bilateral	
Precuneus		Right
Cuneus		Left

Note: *K* = network density. For group differences in degree, *P* value is based on group comparisons using the area under the curve summary metric for the density (*K*) range listed. *P* values are FDR corrected. Hubs present in each group are indicated by the term in the appropriate column. Bilateral indicates hubs were present in both hemispheres, left or right indicates a hub in corresponding hemisphere only.

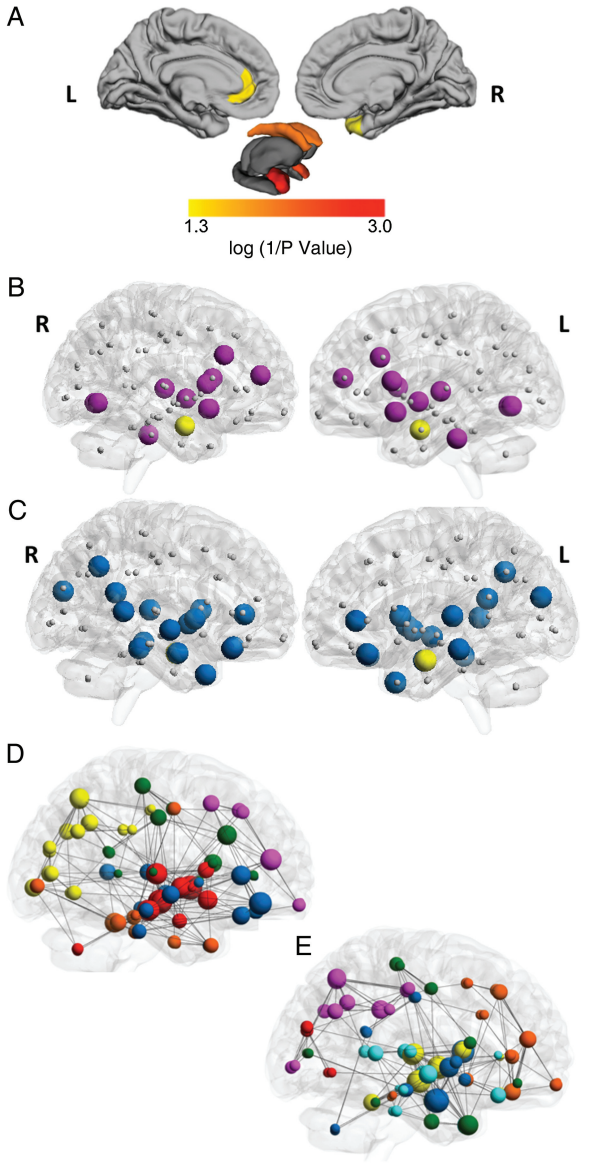

Figure 3. Regional group differences, hubs and modularity. (*A*) Regional group differences in degree are displayed in color on the left lateral and medial cortical surfaces (top row), and on a model of subcortical structures (bottom row). Color indicates regions for which the FXS group demonstrated significantly reduced degree relative to the TD group ($P < 0.05$). There were no regions for which the FXS group demonstrated significantly increased degree. (*B*) Hubs based on degree for the FXS group and (*C*) the TD group. Nodes are shown in gray. Group-specific hubs are shown in purple for the FXS group and blue for the TD group. Common hubs are yellow. Nodes and hubs are displayed on lateral transparent surface rendering of right and left hemispheres. (*D*) Modularity for the fragile X group and (*E*) the TD group. Each color indicates a unique module within each group. Modules are displayed on transparent surface rendering of the right hemisphere.

normalized clustering to normalized path length) was significantly lower for the FXS group, indicating unbalanced network organization. The lower clustering in the FXS network suggests reduced local segregation, a shift toward randomness and less optimal information transfer across the network.

Deficits in global network organization, a novel finding for FXS, could represent the proximal cause of cognitive and behavioral symptoms in this disorder. The distal cause of cognitive/behavioral symptoms is limited or lack of FMRP, which itself is the result of hypermethylation of the *FMR1* promoter region (Oostra and Chiurazzi 2001). Reduced/absent FMRP has been shown to result in altered dendritic spine formation and reduced synaptic plasticity (Swanger and Bassell 2011), both of which lead to decreased synaptic transmission and altered communication at the neuronal level. Our results suggest that limited or lack of FMRP is also associated with alterations of neural systems, evidenced by reduced small-world index. This allows us to infer the effects of FMRP on structural brain network topology and further elucidates the brain basis for cognitive and behavioral symptoms associated with FXS. Structural correlation data are currently only able to yield group-level results, thus, relationships between network measures and cognitive/behavioral measures cannot be explored in the present study. However, altered network dynamics (e.g., measured using functional MRI or diffusion weighted imaging) could be used to develop a connectome-level biological signature for FXS.

The FXS network was also characterized by altered regional network properties, hub locations and modularity, suggesting that network differences exist across multiple levels of network hierarchy. Importantly, group differences in nodal degree and

Table 3 Group differences in cortical thickness

Region	Max log 1/P value	Size (mm^2)	X	Y	Z	Cluster-wise P value (FXS > TD)
Left hemisphere cortical thickness						
Lateral occipital	10.642	15600.66	−23	−93.6	15.3	0.0001
Transverse temporal	5.046	957.75	−35.6	−27	9	0.0169
Superior temporal	4.765	1157.08	−58.7	−10.9	−1.9	0.0047
Pars opercularis	4.372	854.73	−53.4	18.5	16.1	0.0349
Superior frontal	3.609	3065.15	−6.7	24.3	49.7	0.0001
Right hemisphere cortical thickness						
Peri calcarine	7.718	17293.11	11.5	−81.1	12.9	0.0001
Superior frontal	5.11	1348.63	10.9	62.4	8.6	0.0013

Note: Group differences (FXS > TD) in cortical thickness based on Freesurfer qdec comparison (cortical regions). Only significant clusters are listed, statistical threshold was $P < 0.05$ corrected for multiple comparisons using Monte Carlo simulation.

Table 4 Group differences in subcortical/cerebellar volume

	F value	P (FXS > TD)
Subcortical and cerebellar volume		
Left cerebellum cortex	0.440	0.509
Left thalamus	1.214	0.273
Left caudate	29.826	<0.001*
Left putamen	0.253	0.616
Left pallidum	10.586	0.002*
Left hippocampus	0.004	0.947
Left amygdala	0.300	0.585
Left accumbens area	7.813	0.006
Left ventral DC	1.514	0.222
Right cerebellum cortex	1.296	0.258
Right thalamus	0.844	0.361
Right caudate	38.164	<0.001*
Right putamen	0.453	0.502
Right pallidum	4.559	0.035
Right hippocampus	1.040	0.310
Right amygdala	1.843	0.178
Right accumbens area	8.436	0.005
Right ventral DC	0.034	0.855

Note: Group differences (FXS > TD) in subcortical/cerebellar volume based on region of interest comparison. Statistical threshold was $P < 0.003$ (0.05/18 regions). There were no regions for which the FXS group demonstrated significantly reduced volume relative to the TD group.

hub locations provided convergent evidence that bilateral caudate, left amygdala, left rostral anterior cingulate, and right temporal pole were less interactive in the FXS network. Amygdala and caudate are known to display neuroanatomical (Gothelf et al. 2008; Bray et al. 2011), neurofunctional (Menon et al. 2004), and, in the case of the caudate, neurochemical (Bruno et al. 2013) differences in individuals with FXS. The caudate (in conjunction with frontal lobe) is involved in executive functions(Provost et al. 2010); therefore, observed differences in this region may underlie executive function deficits in individuals with FXS. The amygdala (again, in conjunction with frontal lobe) plays a critical role in social cognition (Adolphs 2001) suggesting differences in this region may underlie aberrant social behavior in individuals with FXS. Differences in functional activation of the anterior cingulate, another region involved with social cognition, have been described in individuals with FXS (Bruno et al. 2014). Abnormalities specific to the right temporal pole have not been reported; yet temporal lobe abnormalities in general have been demonstrated (Gothelf et al. 2008; Hoeft et al. 2010). Furthermore, our current univariate results demonstrate cortical thickness difference in bilateral temporal lobes. Absent hubs were also noted in the insula and STS, additional regions critical for social cognition and regions for which individuals with FXS have structural (Cohen et al. 2011) and functional (Garrett et al. 2004) differences. The lack of a FXS group hub in the precuneus may be related to aberrant functional connectivity within the precuneus (self-referential processing) network noted previously in individuals with FXS (Hall et al. 2013). Understanding altered network interaction of these and other regions may help elucidate the nature of network disruptions and, ultimately, how network level disruptions influence cognition and behavior.

Modularity analysis indicates that FXS and TD groups' networks decompose into different sets of interconnected sub networks (Fig. 3 D and E, Supplementary Fig. 3 and Videos 1 and 2). These qualitative between-group differences illuminate specific subnetworks that may represent sites of aberrant local interconnectivity. Of particular interest is the subcortical module in individuals with FXS (red, see Supplementary Fig. 3), which includes all but one of the subcortical structures and no cortical structures. In TD individuals, the subcortical structures are part of several modules including cortical and subcortical structures (e.g., yellow, blue, and green modules). The absence of cortico-subcortical modules is consistent with studies showing aberrant functioning (Menon et al. 2004) and white matter connectivity (Barnea-Goraly et al. 2003) within cortico-subcortical circuits in individuals with FXS. However, recent findings by our group (Green et al. 2015) suggest that the FMR1 gene mutation is associated with increased fiber density. It is important to note that in this previous study the increased fiber density was found in individuals with FXS relative to a group comprised of individuals with developmental disorders (a symptom-matched comparison group) whereas we compare individuals with FXS to an age-matched group of TD individuals. The choice of comparison group is important and future investigations of network topology in FXS would benefit from including both age-matched and symptom-matched comparison groups. While there was significant overlap in the participants with FXS included in the present study and those included in Green et al. 2015 the difference in comparison groups utilized prevent cross study replication and yield complementary interpretations.

The modular organization in the TD group shows overlap with that described previously for cortical thickness networks (Chen et al. 2008) indicating that, in addition to following a small-world architecture, networks including cortical thickness and subcortical volume demonstrate comparable modular organization when compared with the more commonly used cortical

thickness only networks. Our orange module, comprised of several frontal regions, overlaps with the previous executive control module; our pink module includes parietal regions overlapping with the previous sensory motor module; and our light blue module includes temporal regions corresponding to the previous auditory/language module. The coarser cortical parcellation (54 vs. 68) and lack of subcortical nodes in (Chen et al. 2008) limit correspondence between the 2 sets of results. Our results underscore the importance of subcortical structures in characterizing the brain basis of FXS. Furthermore, inclusion of subcortical and cerebellar regions yields a richer network thereby improving our understanding of network dynamics in general. We also performed a secondary graph analysis using cortical volume and subcortical/cerebellar volume and found no significant group differences in global metrics (all P's >0.10). Previous research has reported different patterns of group differences for networks created using different brain morphology metrics (Hosseini et al. 2013), thus this result is not contradictory to our main results. Given the strong evidence for cortical thickness networks relating to structural connectivity (He et al. 2007; Bernhardt et al. 2011) and the superiority of thickness as an endophenotype for neurogenetic syndromes (Panizzon et al. 2009) we limit our interpretations and conclusions to those networks created from cortical thickness and subcortical/cerebellar volume.

Univariate statistical analyses demonstrated increased cortical thickness for the FXS group relative to individuals with TD in frontal, temporal and occipital lobes and greatly enlarged caudate nucleus bilaterally, corresponding with previous investigations (Gothelf et al. 2008; Meguid et al. 2012). Increased thickness and enlarged volume are consistent with our previous reports of altered brain development trajectories in overlapping participants with FXS (Bray et al. 2011) potentially resulting from aberrant synaptic activity and altered dendritic pruning. These group differences remained largely similar when a total brain covariate was added to the model (see Supplementary Fig. 2 and Table 3). Although the extent of significant clusters was reduced when the covariate was added, these results indicate that increased cortical thickness is, to some degree, irrespective of total brain size in FXS.

The cognitive and behavioral symptoms associated with FXS overlap with those associated with ASD (Gabis et al. 2011), yet neuroimaging research indicates a distinct neurobiological signature for each disorder (Hazlett et al. 2009). Connectomic studies of ASD indicate some network alterations including functional networks (created from fMRI data) with reduced clustering and reduced path length but no difference in small-world index (Rudie et al. 2013). Functional networks created from electroencephalography data demonstrated reduced clustering and increased path length in individuals with ASD (Barttfeld et al. 2011). Although, one study indicated that unlike networks in FXS, ASD-related global network differences may not extend to structural networks (Rudie et al. 2013). The altered network pattern we demonstrate in FXS is different from the pattern of network alterations in ASD but, methodological differences such as diffusion (Rudie et al. 2013) versus structural covariance networks for the present study as well as functional networks in both of the aforementioned ASD studies should be noted. Graph theoretical research demonstrating correspondence between functional and structural networks is based on healthy, TD individuals (Hagmann et al. 2008; Hosseini and Kesler 2013a) and the same correspondence should not be assumed in clinical populations. Assessment of functional brain networks in individuals with FXS would help clarify the full impact of reduced FMRP on the human connectome. Studies directly comparing individuals with FXS to those with ASD will be useful for bearing out differences in global and regional network organization and may be essential to pinpoint unique treatment mechanisms despite overlap of cognitive and social symptoms between these disorders. Furthermore, examining network dynamics in FXS relative to groups with other neurodevelopmental disorders including ASD could help specify which altered network properties are specific to FXS and which are more generally related to developmental delay. IQ did not meet the statistical assumptions required to include it as a covariate in the present study; in particular, there was a significant group difference in IQ. Furthermore, including IQ as a covariate in studies of neurodevelopmental disorders often produces overcorrected and counterintuitive results (Dennis et al. 2009).

Structural correlation networks created from thickness/volumetric data correspond with structural connections drawn from diffusion weighted tractography (He et al. 2007) and yield complementary important information (Gong et al. 2012); however, the thickness/volume approach is inherently limited because network measures are computed at the group level. Therefore, we could not examine individual variation in network properties nor could we examine the relationship between individual network properties and clinical measures. A recent paper from our group (Saggar et al. 2015) used a complementary analysis to demonstrate that, in individuals with FXS, individual contribution to group-level structural correlation networks was significantly related to FMRP and to IQ. Future studies with larger sample sizes may utilize subgroup analysis (e.g., compare high functioning vs. low functioning groups) as an alternative method to address relationships between clinical variables and network properties. Furthermore, network analyses of diffusion based structural networks and functional brain networks will be extremely useful for exploring individual differences in network dynamics and their relationship with clinical measures.

The timing of the cognitive/behavioral assessments (within 6 months for all individuals with the exception of 2 in the TD group) represents another limitation; however, we utilize these metrics to describe and characterize our study groups and do not directly relate them to the neuroimaging data. Thus it is a minor limitation.

The present study revealed altered correlation network topology in a broad sample of individuals with FXS, including females and males. Females, like males with FXS, have reduced FMRP, and cognitive and behavioral symptoms, albeit to a lesser degree than their male counterparts (Reiss and Dant 2003). Our sample size was not adequate to undertake analysis separately within sex, yet our results were covaried to control for overall sex effects. Our results were also covaried to control for effects of age within group yet the wide age range somewhat limits our interpretation. Therefore, we performed parallel analyses for a subgroup of our sample over age 15 (Supplementary Table 2) confirming the same pattern of between-group differences in global network topology within this narrower age range. Future developmental studies will be required to determine age-related developmental changes in small-world network topology.

Our primary result, reduced small-worldness in the FXS group, indicates disruption in whole-brain network organization and could help enhance our understanding of the brain basis for cognitive and behavioral symptoms in this important neuropsychiatric disorder. Decreased clustering signifies a connectome shift toward randomness, a finding qualitatively similar to what has been found in examinations of ASD. Altered regional network properties and differences in hubs/modularity may be used to conceptualize how specific regions contribute to overall

network differences in individuals with FXS and they further highlight the importance of subcortical region alterations in the neurobiological signature of FXS. These findings advance our understanding of the effects of FMRP on large-scale brain networks and could be used to develop a connectome-level biological signature for FXS.

Supplementary Material

Supplementary material can be found at: http://www.cercor.oxfordjournals.org/online.

Funding

This work was supported by the National Institutes of Health (NIH5R01-MH50047 to A.L.R., T32-MH19908 to A.L.R., J.L.B., and K99-MH104605 to M.S.); the Fonds de Recherche Société et Culture Québec (E.M.Q.); and the Canel Family Research Fund.

Notes

We wish to sincerely thank the families who participated in this research. *Conflict of Interest*: A.L.R. disclosed personal fees from Genentech outside the submitted work. J.L.B., S.M.H.H., M.S., E.M.Q., and M.M.R. reported no biomedical financial interests or potential conflicts of interest.

Author Contributions

J.L.B. had full access to all of the data in the study and takes responsibility for the integrity of the data and the accuracy of the data analysis. J.L.B. carried out the statistical analysis and drafted the manuscript. A.L.R. conceived of the study, participated in its design and coordination and helped to draft the manuscript. S.M.H.H. and M.S. contributed to the graph theoretical analysis and helped to draft the manuscript. E.M.Q. recruited participants, collected the data and helped to analyze the data and draft the manuscript. M.M.R. performed the preprocessing of anatomical images and helped to draft the manuscript. All authors read and approved the final manuscript.

References

Adolphs R. 2001. The neurobiology of social cognition. Curr Opin Neurobiol. 11:231–239.

Alexander-Bloch A, Raznahan A, Bullmore E, Giedd J. 2013. The convergence of maturational change and structural covariance in human cortical networks. J Neurosci. 33:2889–2899.

Aman MG, Burrow WH, Wolford PL. 1995. The aberrant behavior checklist-community—factor validity and effect of subject variables for adults in group homes. Am J Ment Retard. 100:283–292.

Barnea-Goraly N, Eliez S, Hedeus M, Menon V, White CD, Moseley M, Reiss AL. 2003. White matter tract alterations in fragile X syndrome: preliminary evidence from diffusion tensor imaging. Am J Med Genet. 118B:81–88.

Barttfeld P, Wicker B, Cukier S, Navarta S, Lew S, Sigman M. 2011. A big-world network in ASD: dynamical connectivity analysis reflects a deficit in long-range connections and an excess of short-range connections. Neuropsychologia. 49:254–263.

Bassett DS, Bullmore E, Verchinski BA, Mattay VS, Weinberger DR, Meyer-Lindenberg A 2008. Hierarchical organization of human cortical networks in health and schizophrenia. J Neurosci. 28:9239–9248.

Bernhardt BC, Chen Z, He Y, Evans AC, Bernasconi N. 2011. Graph-theoretical analysis reveals disrupted small-world organization of cortical thickness correlation networks in temporal lobe epilepsy. Cereb Cortex. 21:2147–2157.

Bray S, Hirt M, Jo B, Hall SS, Lightbody AA, Walter E, Chen K, Patnaik S, Reiss AL. 2011. Aberrant frontal lobe maturation in adolescents with fragile X syndrome is related to delayed cognitive maturation. Biol Psychiatry. 70:852–858.

Bruno J, Shelly E, Quintin E-M, Rostami M, Patnaik S, Spielman D, Mayer D, Gu M, Lightbody AA, Reiss AL. 2013. Aberrant basal ganglia metabolism in fragile X syndrome: a magnetic resonance spectroscopy study. J Neurodev Disord. 5:20.

Bruno JL, Garrett AS, Quintin E-M, Mazaika PK, Reiss AL. 2014. Aberrant face and gaze habituation in fragile X Syndrome. Am J Psychiatry. 171:1099–1106.

Chen ZJ, He Y, Rosa-Neto P, Germann J, Evans AC. 2008. Revealing modular architecture of human brain structural networks by using cortical thickness from MRI. Cereb Cortex. 18:2374–2381.

Cohen JD, Nichols T, Brignone L, Hall SS, Reiss AL. 2011. Insular volume reduction in fragile X syndrome. Int J Dev Neurosci. 29:489–494.

Dale A, Fischl B, Sereno MI. 1999. Cortical surface-based analysis: I. segmentation and surface reconstruction. Neuroimage. 9:179–194.

Dennis M, Francis DJ, Cirino PT, Schachar R, Barnes MA, Fletcher JM. 2009. Why IQ is not a covariate in cognitive studies of neurodevelopmental disorders. J Int Neuropsychol Soc. 15:331.

Gabis LV, Baruch YK, Jokel A, Raz R. 2011. Psychiatric and autistic comorbidity in fragile X syndrome across ages. J Child Neurol. 26:940–948.

Garrett AS, Menon V, Mackenzie K, Reiss AL. 2004. Here's looking at you, kid. JAMA Psychiatry. 61:281–288.

Gonçalves JT, Anstey JE, Golshani P, Portera-Cailliau C. 2013. Circuit level defects in the developing neocortex of fragile X mice. Nat Neurosci. 16:903–909.

Gong G, He Y, Chen ZJ, Evans AC. 2012. Convergence and divergence of thickness correlations with diffusion connections across the human cerebral cortex. Neuroimage. 59:1239–1248.

Gothelf D, Furfaro JA, Hoeft F, Eckert MA, Hall SS, O'Hara R, Erba HW, Ringel J, Hayashi KM, Patnaik S, et al. 2008. Neuroanatomy of fragile X syndrome is associated with aberrant behavior and the fragile X mental retardation protein (FMRP). Ann Neurol. 63:40–51.

Green T, Barnea-Goraly N, Raman M, Hall SS, Lightbody AA, Bruno JL, Quintin E-M, Reiss AL. 2015. Specific effect of the fragile-X mental retardation-1 gene (FMR1) on white matter microstructure. Br J Psychiatry. 207:143–148.

Hagmann P, Cammoun L, Gigandet X, Meuli R, Honey CJ, Wedeen VJ, Sporns O. 2008. Mapping the structural core of human cerebral cortex. PLoS Biol. 6:e159.

Hall SS, Burns DD, Lightbody AA, Reiss AL. 2008. Longitudinal changes in intellectual development in children with fragile X syndrome. J Abnorm Child Psychol. 36:927–939.

Hall SS, Jiang H, Reiss AL, Greicius MD. 2013. Identifying large-scale brain networks in fragile X syndrome. JAMA Psychiatry. 70:1215.

Hazlett HC, Poe MD, Lightbody A a., Gerig G, MacFall JR, Ross AK, Provenzale J, Martin A, Reiss AL, Piven J. 2009. Teasing apart the heterogeneity of autism: same behavior, different brains in toddlers with fragile X syndrome and autism. J Neurodev Disord. 1:81–90.

He Y, Chen Z, Evans A. 2008. Structural insights into aberrant topological patterns of large-scale cortical networks in Alzheimer's disease. J Neurosci. 28:4756–4766.

He Y, Chen ZJ, Evans AC. 2007. Small-world anatomical networks in the human brain revealed by cortical thickness from MRI. Cereb Cortex. 17:2407–2419.

Hirschberger M, Qi Y, Steuer RE. 2007. Randomly generating portfolio-selection covariance matrices with specified distributional characteristics. Eur J Oper Res. 177:1610–1625.

Hoeft F, Carter JC, Lightbody AA, Cody Hazlett H, Piven J, Reiss A.L. 2010. Region-specific alterations in brain development in one- to three-year-old boys with fragile X syndrome. Proc Natl Acad Sci. 107:9335–9339.

Hosseini SM, Koovakkattu D, Kesler SR. 2012. Altered small-world properties of gray matter networks in breast cancer. BMC Neurol. 12:28.

Hosseini SMH, Black JM, Soriano T, Bugescu N, Martinez R, Raman MM, Kesler SR, Hoeft F. 2013. Topological properties of large-scale structural brain networks in children with familial risk for reading difficulties. Neuroimage. 71:260–274.

Hosseini SMH, Hoeft F, Kesler SR. 2012. GAT: A Graph-Theoretical Analysis Toolbox for analyzing between-group differences in large-scale structural and functional brain networks. PLoS ONE. 7:e40709.

Hosseini SMH, Kesler SR. 2013a. Comparing connectivity pattern and small-world organization between structural correlation and resting-state networks in healthy adults. Neuroimage. 78:402–414.

Hosseini SMH, Kesler SR. 2013b. Influence of choice of null network on small-world parameters of structural correlation networks. PLoS ONE. 8:e67354.

Humphries M, Gurney K, Prescott T. 2006. The brainstem reticular formation is a small-world, not scale-free, network. Proc R Soc B Biol Sci. 273:503–511.

Irwin SA, Patel B, Idupulapati M, Harris JB, Crisostomo RA, Larsen BP, Kooy F, Willems PJ, Cras P, Kozlowski PB, et al. 2001. Abnormal dendritic spine characteristics in the temporal and visual cortices of patients with fragile-X syndrome: a quantitative examination. Am J Med Genet. 98:161–167.

Kaiser M, Hilgetag CC. 2006. Nonoptimal component placement, but short processing paths, due to long-distance projections in neural systems. PLoS Comput Biol. 2:0805–0815.

Lee AD, Leow AD, Lu A, Reiss AL, Hall S, Chiang M-C, Toga AW, Thompson PM. 2007. 3D pattern of brain abnormalities in Fragile X syndrome visualized using tensor-based morphometry. Neuroimage. 34:924–938.

Leow A, Harvey D, Goodrich-hunsaker NJ, Gadelkarim J, Kumar A, Zhan L, Rivera SM, Simon TJ. 2014. Altered structural brain connectome in young adult fragile X premutation carriers. Hum Brain Mapp. 4530:4518–4530.

Meguid NA, Fahim C, Sami R, Nashaat NH, Yoon U, Anwar M, El-Dessouky HM, Shahine EA, Ibrahim AS, Mancini-Marie A, et al. 2012. Cognition and lobar morphology in full mutation boys with fragile X syndrome. Brain Cogn. 78:74–84.

Menon V, Leroux J, White CD, Reiss AL. 2004. Frontostriatal deficits in fragile X syndrome: relation to FMR1 gene expression. Proc Natl Acad Sci U S A. 101:3615–3620.

Newman M. 2006. Modularity and community structure in networks. Proc Natl Acad Sci. U S A 103:8577–8582.

O'Brien LM, Ziegler DA, Deutsch CK, Frazier JA, Herbert MR, Locascio JJ. 2011. Statistical adjustments for brain size in volumetric neuroimaging studies: some practical implications in methods. Psychiatry Res Neuroimaging. 193:113–122.

Oostra BA, Chiurazzi P. 2001. The fragile X gene and its function. Clin Genet. 60:399–408.

Panizzon MS, Fennema-Notestine C, Eyler LT, Jernigan TL, Prom-Wormley E, Neale M, Jacobson K, Lyons MJ, Grant MD, Franz CE, et al. 2009. Distinct genetic influences on cortical surface area and cortical thickness. Cereb Cortex. 19:2728–2735.

Peng DX, Kelley RG, Quintin E, Raman M, Thompson PM, Reiss AL. 2014. Cognitive and behavioral correlates of caudate subregion shape variation in fragile X syndrome. Hum Brain Mapp. 2868:2861–2868.

Provost J-S, Petrides M, Monchi O. 2010. Dissociating the role of the caudate nucleus and dorsolateral prefrontal cortex in the monitoring of events within human working memory. Eur J Neurosci. 32:873–880.

Reiss AL, Dant CC. 2003. The behavioral neurogenetics of fragile X syndrome: analyzing gene-brain-behavior relationships in child developmental psychopathologies. Dev Psychopathol. 15:927–968.

Rubinov M, Sporns O. 2010. Complex network measures of brain connectivity: uses and interpretations. Neuroimage. 52:1059–1069.

Rubinov M, Sporns O. 2011. Weight-conserving characterization of complex functional brain networks. Neuroimage. 56:2068–2079.

Rudie JD, Brown JA, Beck-Pancer D, Hernandez LM, Dennis EL, Thompson PM, Bookheimer SY, Dapretto M. 2013. Altered functional and structural brain network organization in autism. NeuroImage Clin. 2:79–94.

Saggar M, Hosseini SMH, Bruno JL, Quintin E, Raman MM, Kesler SR, Reiss AL. 2015. NeuroImage Estimating individual contribution from group-based structural correlation networks. Neuroimage. 120:274–284.

Sporns O. 2011. The human connectome: a complex network. Ann N Y Acad Sci. 1224:109–125.

Swanger SA, Bassell GJ. 2011. Making and breaking synapses through local mRNA regulation. Curr Opin Genet Dev. 21:414–421.

Watts DJ, Strogatz SH. 1998. Collective dynamics of "small-world" networks. Nature. 393:440–442.

Wechsler D. 1991. WISC-III: Wechsler intelligence scale for children, 3rd edn. San Antonio (TX): Psychological Corporation.

Wechsler D. 1997. Wechsler adult intelligence scale, 3rd ed. San Antonio (TX): Harcourt Assessment.

Willemsen R, Smits A, Mohkamsing S, Van Beerendonk H, De Haan A, De Vries B, Van Den Ouweland A, Sistermans E, Galjaard H, Oostra BA. 1997. Rapid antibody test for diagnosing fragile X syndrome: a validation of the technique. Hum Genet. 99:308–311.

Xia M, Wang J, He Y. 2013. BrainNet viewer : a network visualization tool for human brain connectomics. PLoS ONE. 8:e68910.

Zalesky A, Fornito A, Bullmore E. 2012. On the use of correlation as a measure of network connectivity. Neuroimage. 60:2096–2106.